Contents lists available at ScienceDirect

Arabian Journal of Chemistry

journal homepage: www.ksu.edu.sa

Original article

Naoxintong capsules exhibited a protective effect against cerebral ischemia in the brain hub region of MCAO rats via intervention of amino acid metabolism

Huanhuan Wang [a,b,1], Jingtong Liu [a,1], Mengli Chang [a,1], Guanghuan Tian [a], Xixian Kong [a], Mengting Liu [d], Na Guo [c], Liying Tang [a], Jing Xu [a,*], Hongwei Wu [a,*], Hongjun Yang [c]

[a] Institute of Chinese Materia Medica, China Academy of Chinese Medical Sciences, Beijing 100700, China
[b] Hospital of Integrated Chinese and Western Medicine, Tianjin university of TCM, Tianjin 300100, China
[c] Experimental Research Centre, China Academy of Chinese Medical Sciences, Beijing 100700, China
[d] Zhejiang Chinese Medical University, Zhejiang Province 310053, China

ARTICLE INFO

Keywords:
Cerebral ischemia
Amino acids
LC-QQQ-MS
Naoxintong capsules
Metabonomic

ABSTRACT

Background: Amino acids (AAs) metabolism profiles in brain play a pivotal role in cerebral ischemia (CI), which is a complex, spatial and temporal event. NaoXinTong Capsules (NXT) are widely prescribed in Chinese medicine for the treatment of cerebrovascular and cardiovascular diseases.
Methods: In this study, a novel analytical method for the quantification of twenty-three AAs in cortex and hippocampus was developed by UPLC-QQQ-MS. Based on middle cerebral artery occlusion (MCAO) rat model, the cerebral infarction and the neurological behavior scores are firstly dynamically evaluated at 3, 12, and 24 h after CI. Then the dynamic levels of the AAs in cortex and hippocampus were analyzed respectively after CI.
Results: After CI, MCAO rats showed neurological deficits especially at 24 h. Based on PCA scores plot at different time after CI, the time of the AAs metabolism showing an obvious disturbance in the cortex (12 and 24 h after ischemia) is earlier than that in the hippocampus (24 h after ischemia). Based on the fold-changes of MCAO vs. sham group and receiver operating curve (ROC) analysis, a total of nine AAs biomarkers, with continuous and consistent changes at different time points after CI, were finally obtained including eight AAs of Ala, GABA, Pro, Val, Ile, His, Cit and Leu in the cortex, and three AAs of Ile, Asp, and Cit in the hippocampus. After NXT treatment, the efficacy was confirmed by reducing cerebral infarction and improving the neurological behavior scores. Furthermore, GABA, Pro, His, Leu, Asp, Ile and Cit were found to exhibited an obvious tendency for returning to baseline values in the corresponding regions at 24 h after CI ($P < 0.05$).
Conclusion: This study provides new strategies to explore the mechanism of CI and help discover the potential mechanism of NXT.

1. Introduction

As a medical emergency, stroke is the primary cause of death and adult disability worldwide(Zhou et al., 2018). In all stroke cases, approximately 87 % are caused by cerebral ischemia (CI)(Jangholi et al., 2020; Jiang and Yu, 2021). As the ischemic time advances, the lack of blood supply deprives the brain cells of necessary glucose and oxygen, and disturbs cellular homeostasis, inducing metabolic changes(Xing et al., 2012). Since the different neuronal subpopulations have different patterns or levels of susceptibility and tolerance, and thus, the metabolite response to global cerebral ischemia is region specific(Jurkowski et al., 2020; Mitani et al., 1993; Rho et al., 2018). CI typically results in

Abbreviations: CI, cerebral ischemia; NXT, Naoxintong capsules; MCAO, middle cerebral artery occlusion; AAs, amino acid; ROC, receiver operating curve; Ala, alanine; Ser, serine; Pro, proline; Val, valine; Thr, threonine; Cys, cysteine; Tau, taurine; Hyp, hydroxyproline; Ile, isoleucine; Asp, aspartate; Homo-CYS, homocysteine; Gln, glutamine; Glu, glutamate; Met, methionine; His, histidine; Phe, phenylalanine; Arg, arginine; Cit, citrulline; Try, tryptophan; Gly, glycine; Leu, leucine; Lys, lysine; Tyr, tyrosine; BCAAs, branched chain amino acids.

* Corresponding authors.
E-mail addresses: jxu0930@icmm.ac.cn (J. Xu), hwwu@icmm.ac.cn (H. Wu).
[1] These authors contributed equally to this work.

https://doi.org/10.1016/j.arabjc.2024.105659
Received 23 August 2023; Accepted 28 January 2024
Available online 1 February 2024

extensive damage in the ischemic cortex and hippocampal CA1 area neurons(Klacanova et al., 2019; Song et al., 2018; Wahul et al., 2018; Wang et al., 2015), and the possible mechanisms include excitotoxicity, oxidative stress, and inflammation.

Amino acid (AAs) act as essential neurotransmitters to control and regulate cerebral activity, especially the excitotoxicity induced by the release of a large amount of excitatory amino acids at the hyperacute phase of ischemic stroke, which is one of mechanisms underlying ischemic brain injury and nerve cell death(Bame et al., 2014; Muir and Lees, 2003; Zhu et al., 2015). Therefore, it is crucial to investigate the dynamic changes in AAs for the protection of neurons and treatment translation research at the hyperacute phase of ischemic stroke. AAs as important biomarkers of cerebral ischemia has been deeply studied (Guan et al., 2014; Igarashi et al., 2015; Liu et al., 2016b; Wang et al., 2014). However, previous studies were mostly based on a single time and lacked dynamic analysis in the different special regions of brain after CI. There are some inconsistent reports of the changing of AAs biomarkers after CI, which attributes to the differences in sampling time, the specificity of the detected regions in the brain, and the errors caused by different analysis methods(Liu et al., 2016b). Quantitative analysis of AAs in biological samples is a traditional technology. HPLC-MS is the most used detection technique for AAs analyses because of its high sensitivity, high selectivity and without derivatization. Although there are some reports about the detection of AAs in biological sample by HPLC-MS/MS, the number of AAs detected in cortex and hippocampus was fewer and limited which cannot fully reflect dynamic changes of the levels of AAs in cortex and hippocampus.

Traditional Chinese medicine (TCM) has the advantage of overall regulation in treating CI. Naoxintong capsules (NXT), derived from a classical TCM formulation Bu-Yang-Huan-Wu-Tang, are widely used to treat cerebrovascular and cardiovascular diseases in China(Chen et al., 2014; Haiyu et al., 2016; Liang et al., 2018; Zhao et al., 2018), which consists of 16 various kinds of TCM herbs or animal powders. Previous studies have shown that NXT has protective effects in stroke and cardiovascular diseases, such as anti-atherosclerosis, antioxidant, regulating energy metabolism and so on(Chen et al., 2012, 2011; Zhang et al., 2013; Zhong et al., 2013). Our previous study has found NXT exhibited a neuroprotective effect by regulating amino acid metabolism in the cerebrospinal fluid of ischemic rats. However, the dynamic changes of amino acid metabolism profiles in cortex and hippocampus after ischemia and the intervention mechanism of NXT remains unclear.

In this study, a rapid, sensitive, accurate, and specified method for the quantification of twenty three AAs without derivatization in cortex and hippocampus was developed by UPLC-QQQ-MS. Based on a middle cerebral artery occlusion (MCAO) rat model, the dynamic levels of the AAs in cortex and hippocampus were analyzed respectively at 3, 12 and 24 h after CI in an effort to discovery the relations between the changes of the levels of AAs and development of ischemic injury in the acute phase, as well as intervention mechanism of NXT. In order to accurately discovery the credible AAs biomarkers related to the development of ischemic injury, the fold-changes (MCAO group vs. sham group) based on the contents of all detected AAs was firstly used to filtered the potential biomarkers, those have a continuous and consistent changing trend at different time points after CI. Then based on the these, receiver operating curve (ROC) analysis was further conducted to evaluate the diagnostic value of these continuously changing AAs and confirm the credible AAs biomarkers. The overall experimental procedure of this study is shown in Graph abstract.

2. Materials and methods

2.1. Animals, chemicals and reagents

Adult male Sprague-Dawley rats weighing 260 ± 10 g were obtained from the Animal Breeding Centre of Beijing Vital Rver Laboratories Company (Beijing, China). All animals were housed at 22 ± 2 °C with a relative humidity of 50 ± 10 % and a 12 h light/12 h dark cycle. The animals had free access to water and fodder (Beijing Keaoxieli Co., Ltd.). All experimental animal procedures were approved by the China Academy of Chinese Medical Sciences' Administrative Panel on Laboratory Animal Care and performed in accordance with institutional guidelines and ethics of the committee as part of the China Academy of Chinese Medical Sciences (code, ERCCACMS21-2111–02). Twenty-three AA standards, including alanine, GABA, Ser, Pro, Val, Thr, Hyp, Ile, Asp, Gln, Glu, Met, His, Phe, Arg, Cit, Trp, Gly, His, Leu, Lys, Tyr (purity > 99 %, all), and acrylamide-d3 (internal standard (IS)), were purchased from Sigma-Aldrich (St. Louis, MO, USA). Acetonitrile, methanol, formic acid, and ammonium formate were provided by Fisher Scientific (Shanghai, China). All chemicals used throughout this study were of HPLC grade unless stated otherwise. NXT (batch number: 140156) was provided by Buchang Pharma Co., Ltd.

2.2. MCAO surgery and drug administration

A total of 108 rats were randomly divided into three groups: sham operation (sham), MCAO model group with water treatment (MCAO), and MCAO group with NXT treatment (NXT, 110 $mg{\cdot}kg^{-1}{\cdot}d^{-1}$ dosages). The MCAO group was randomly divided into the following subgroups: MCAO 3 h (3 h after MCAO), MCAO 12 h (12 h after MCAO) and MCAO 24 h (24 h after MCAO). The sham and NXT groups were also divided into three subgroups according to the surgery time, which was the same as the MCAO subgroups. Twelve rats were involved in each subgroup. A permanent MCAO model was applied in this study. According to a previous description, MCAO surgery was carried out by intraluminal occlusion using a monofilament(Longa et al., 1989; Woitzik et al., 2006; Yamori et al., 1976). The NXT was orally administered twice a day at 8 AM and 8 PM for 5 days. On the sixth day, after administration of NXT for 1 h, the rats were subjected to MCAO. The same procedures were performed except for the occlusion in the sham group. After occlusion for 3, 12 and 24 h, the rats were sacrificed. The brain was obtained for TTC staining, and the hippocampal and cortex tissues of the whole brain were obtained and stored at −80 °C for LC-QQQ-MS analysis.

2.3. Evaluation of the MCAO model and NXT effect

To evaluate the protective effect of NXT against cerebral ischemia, neurological function was evaluated blindly by Longa's Neurological Severity Score(Longa et al., 1989). The brain was cut into 5 coronal sections, and the slices were stained with 0.5 % 2,3,5-triphenyltetrazolium chloride (Sigma, St. Louis, MO, USA) for 15 min at 37 °C. Numerical images were captured, and the infarct volume was calculated as infarct area × thickness (1 mm). The summation of the infarct volumes for all brain slices was defined as the total infarct volume.

2.4. UPLC-QQQ-MS analysis

2.4.1. Chromatographic and mass spectrometric conditions

Chromatographic experiments were performed on a Waters Acquity UPLC (Waters Corporation, Milford, MA, USA) instrument consisting of a dual pump, an online degasser, an autosampler, and a thermostatically controlled column. The column temperature was maintained at 40 °C on an ACQUITY UPLC BEH amide column (100 mm × 21 mm, 1.7 μm, Waters™, USA) with Phenomenex SecurityGuard™ ULTRA. The mobile phase consisted of solvent A (water containing 2 mM ammonium formate and 0.2 % formic acid) and solvent B (acetonitrile containing 0.2 % formic acid) with a gradient elution (85 % A at 0–0.5 min, 85–80 % A at 0.5–1 min, 80–76 % A at 1–5 min, 76–50 % A at 5–5.5 min, and 50–85 % A at 5.5–6 min). The flow rate of the mobile phase was 0.3 mL/min. The autosampler was kept at 4 °C, and the injection volume was 5 μL.

MS analysis was performed on a Waters Xevo TQ-S triple quadrupole equipped with an ESI source in the positive ion mode and detected by

scheduled multiple reaction monitoring (MRM). Ion transitions and retention times for the detection of amino acids are shown in Table 1. Data were acquired using MassLynx 4.1 software and processed by TargetLynx (Waters Corp., Milford, MA, USA). The obtained data were then exported to Excel (2010 Edition, Microsoft Corporation) for further calculations. The compounds were quantified using an internal standard method. The MS parameters for twenty-three AAs and IS are shown in Table 1.

2.4.2. Preparation of standard solutions

Appropriate amounts of twenty-three reference compounds, including Met, GABA, Hyp, Gln, Ala, Trp, Arg, Phe, His, Thr, Asp, Glu, Pro, Ile, Tau, Cit, Val, Ser, Leu, Gly, Lys, Tyr and Histamine were weighed respectively and dissolved in water. Then take different volumes of the standard solutions to prepare the mixed standard stock solution.

2.4.3. Preparation of sample solutions

Hippocampus and cortex samples were thawed and allowed to equilibrate at room temperature prior to analysis. The frozen samples were homogenized in a twenty-fold volume of 20 % methanol, and then, 20 μL homogenates were mixed with 975 μL of the initial mobile phase and 5 μL of IS (Acrylamide-d3, 200 ng/mL). The mixture was then vortexed for 1 min prior to analysis and deproteinized by centrifugation at 4 °C (12000 × g for 5 min), and 5 μL of the supernatant was subjected to UPLC-MS analysis for AAs analysis.

2.4.4. Method validation

(1). Linearity, Sensitivity and Carryover

Stock solutions were all diluted to 0.1 to 1000 ng·mL^{-1} concentrations with the initial mobile phase for the construction of calibration curves and evaluated for linearity. Before injection, 995 μL of each standard was mixed with 5 μL of IS (Acrylamide-d3, 200 ng/mL). Therefore, the content of IS in each standard was the same as in the prepared hippocampus and cortex samples. The calibration equations were determined using the ratio of the twenty-three AA peak areas to the internal standard (acrylamide-d3) peak area. The linearity of the calibration curves was established by the coefficient of determination (R^2). The sensitivity was evaluated using limits of detection (LOD) and limits of quantification (LOQ). The LOD was defined as the concentration at a signal-to-noise (S/N) ratio of 3, and the LOQ was defined at an S/N ratio of 10. As the concentration range of quantitation was wide in this study, carryover was investigated. The procedure of carryover was to inject a vehicle blank sample following the injections of the standards with limit of quantitation (LOQ) concentrations. Significant carryover was defined as a measurable signal in the blanks of > 20 % of the limit of quantification (LOQ) signal.

(2). Precision and Accuracy

The precision of the method was determined by measuring both intra-day precision and inter-day precision. The intra-day precision was investigated with the standard solution samples at intermediate concentration levels. The inter-day precision was similarly evaluated over seven consecutive days. Precision was evaluated by determination of the relative standard deviation (RSD), which was calculated as the ratio of the standard deviations to the mean value of six replicates for the analyzed compounds. The recovery test was used to evaluate the accuracy of the method. The recovery was determined by spiking a selected sample. First, the contents of the detected analytes in the sample were calculated according to their respective calibration curves, before spiking six sample aliquots with about identical amounts of the reference compound mixture. Then, the thus fortified samples were prepared and analyzed as described above. The spike recoveries were calculated by the formula: Spiked recovery (%) = (observed amount − original amount)/spiked amount × 100 %.

(3). Stability and Repeatability

To assess freeze–thaw stability, a series of parallel samples from the same representative sample was subjected to three freeze–thaw cycles consisting of thawing samples at room temperature (15 ~ 20 °C) for at least one hour, vortexing, and then refreezing for at least 12 h at −80 °C. After three freeze–thaw cycles, the samples were analyzed using freshly prepared calibration standards. Considering that the samples were placed in the autosampler for a long waiting time as a consequence of large sample numbers, the short-term stability was evaluated by analyzing the samples that were kept in 4 °C autosampler for 0 and 24 h

Table 1
MS parameters for twenty-three amino acids in ESI + mode.

No.	Amino acids	Formula	Parent (*m/z*)	Daughter (*m/z*)	Cone (V)	Collision (V)	Retention Time(min)
1	Met	$C_5H_{11}NO_2S$	150.0819	104.1260	22	10	2.82
2	GABA	$C_4H_9NO_2$	104.0919	87.0137	32	10	2.60
3	Hyp	$C_5H_9NO_3$	132.0919	86.1515	32	12	4.09
4	Gln	$C_5H_{10}N_2O_3$	147.0381	84.0665	20	14	5.01
5	Ala	$C_3H_7NO_2$	90.0000	44.0000	18	10	1.10
6	Trp	$C_{11}H_{12}N_2O_2$	205.1119	188.1188	40	10	2.44
7	Arg	$C_6H_{14}N_4O_2$	175.1419	70.1507	58	20	6.50
8	Phe	$C_9H_{11}NO_2$	166.1119	120.1065	16	12	2.44
9	His	$C_6H_9N_3O_2$	156.1600	80.6300	25	20	0.97
10	Thr	$C_4H_9NO_3$	120.0181	74.1256	24	10	4.33
11	Asp	$C_4H_7NO_4$	134.0619	88.1097	24	8	5.02
12	Glu	$C_5H_9NO_4$	148.0819	84.0696	20	14	4.43
13	Pro	$C_5H_9NO_2$	116.0919	70.1084	30	12	3.18
14	Ile	$C_6H_{13}NO_2$	132.1219	86.1632	18	10	2.54
15	Tau	$C_2H_7NO_3S$	125.9781	108.0677	44	10	3.27
16	Cit	$C_6H_{13}N_3O_3$	176.1219	159.0612	20	8	5.61
17	Val	$C_5H_{11}NO_2$	106.0081	60.0839	30	8	5.09
18	Ser	$C_3H_7NO_3$	106.0081	60.0839	30	8	2.43
19	Leu	$C_6H_{13}NO_2$	132.0581	86.1637	20	8	2.37
20	Gly	$C_2H_5NO_2$	75.9981	30.1491	30	4	6.55
21	Lys	$C_6H_{14}N_2O_2$	147.0800	84.1500	20	14	3.13
22	Tyr	$C_9H_{11}NO_3$	182.1596	136.1613	28	14	6.37
23	Histamine	$C_5H_9N_3$	111.9681	94.8591	18	12	0.74
24	Acrylamide-d3	$C_3H_2D_3NO$	171.1597	125.0326	22	12	2.53

after preparation, respectively. For the repeatability assay, six independent samples prepared from the homogenate sample were extracted and analyzed in parallel for the evaluation of repeatability. The RSD was taken as a measure of stability and repeatability.

2.5. Data processing and Statistical analysis

The raw data is obtained and aligned using the MassHunter workstation (B0.06.00, Agilent) according to the *m/z* value and retention time of the ion signal. Principal component analysis (PCA) was first used as an unsupervised method to visualize the overall differences for sham, model, and NXT at 3, 12, and 24 h after MCAO. Analysis was performed using SIMCA-P 12.0 software and omicshare (https://www.omicshare.com). The FC (MCAO vs. Sham group and NXT vs. MCAO group) in the cortex and hippocampus at different time points is displayed by a heatmap. Analysis was performed using omicshare (https://www.omicshare.com). ROC analysis was conducted with SPSS software to estimate the predictive potential of the candidate diagnostic biomarkers. The metabolic pathways associated with the identified metabolic markers were then constructed and analyzed using the MetaboAnalyst platform, and the related mechanism of action was explored. A significant pathway was claimed with a false discovery rate corrected $P < 0.05$. Statistical significance was determined by one-way ANOVA followed by Tukey's multiple comparison test or Student's t tests for 2 group comparisons. All values are presented as the means ± sd. A value of $p < 0.05$ was considered statistically significant.

3. Results and discussions

3.1. NXT shows a protective effect against cerebral ischemia in MCAO rats

As shown in Fig. 1A, rats in the sham group did not show neurological deficits, and the neurological function scores of the neurological defect symptoms in the model group were significantly higher than those in the sham group ($p < 0.001$) at 3, 12, and 24 h after MCAO-induced CI injury ($P < 0.05$). Based on previous study, different dosages of NXT against CI have been studied and compared(Liu et al., 2016a). 110 $mg{\cdot}kg^{-1}{\cdot}d^{-1}$ dosages of NXT showed the best effects and therefore were used in this study. NXT significantly reduced the neurological deficit score at 3, 12, and 24 h after MCAO-induced CI injury ($P < 0.05$), indicating improved neurological function in MCAO rats ($p < 0.001$). As shown in Fig. 1B-C, TTC staining was applied for the estimation of cerebral infarction at 12 and 24 h after occlusion of the artery. MCAO-induced ischemia produced a marked infarct area in serial coronal brain sections. However, NXT treatment significantly reduced the infarct area at 12 and 24 h after occlusion of the artery. Overall, NXT was able to significantly reduce neurological deficits and the infarction rate in MCAO rats.

3.2. Method validation

3.2.1. Linearity, sensitivity and carryover

Fig. 2 is the typical overlap extracted ion chromatograms (EIC) of the twenty-three detected AAs in the hippocampus and cortex samples. Each peak of the twenty-three detected AAs has an acceptable shape. The method exhibited excellent sensitivity based on the signal-to-noise (S/N) ratio. The sensitivity investigation of this analytical method is shown in Table 2. For all analytes, the LOD was in the range of 0.002–3000 pg/mL (S/N > 3), and the LOQ was 0.015–30000 pg/mL (S/N > 10). The linear response of the calibration curve was determined by a series of standards with different concentrations. The mean regression coefficients (r) for all the analytes were obtained from 0.894 to 0.999. The results are shown in Table 2, indicating excellent linearity. The calibration ranges were sufficient to cover analyte concentrations in almost all the hippocampus and cortex samples. As for carryover evaluation, the vehicle blank sample injected following the LOQ standard injection has no significant peaks at the retention times of all the analytes. Considering that the carryover measurement can be affected by its position in the sampling sequence due to adsorptive carryover issues, vehicle blank samples were injected at regular intervals (every ten samples) throughout the analytical run. In addition, as the ion pairs including parent ion and daughter ion (as shown in Table 1) detected by MRM between IS and the analytes were all different, there is no significant crosstalk observed between IS and analytes in this method.

3.2.2. Precision and Accuracy

Intra-day and inter-day precisions and accuracies for the mixed standard solution samples are summarized in Table 2. In this study, the intra-day and inter-day precisions were less than 6.10 % and 2.99 % respectively. In the cortex and hippocampus samples, the average recoveries of the detected AAs were between 80.0 % and 129.08 % and the

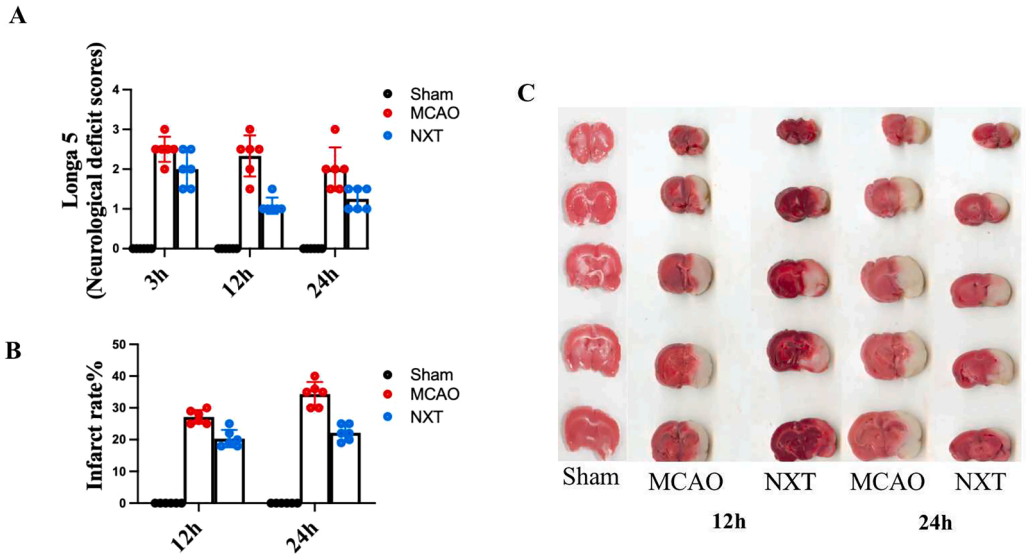

Fig. 1. NXT has significant protective effect on cerebral ischemia. A neurobehavioral score; B infarct area; C TTC staining of the brain. $^{*}p < 0.05$, $^{**}p < 0.01$, and $^{***}p < 0.001$ in the MCAO group versus the sham group; $^{\#}p < 0.05$, $^{\#\#}p < 0.01$, and $^{\#\#\#}p < 0.001$ in the NXT group versus the MCAO group.

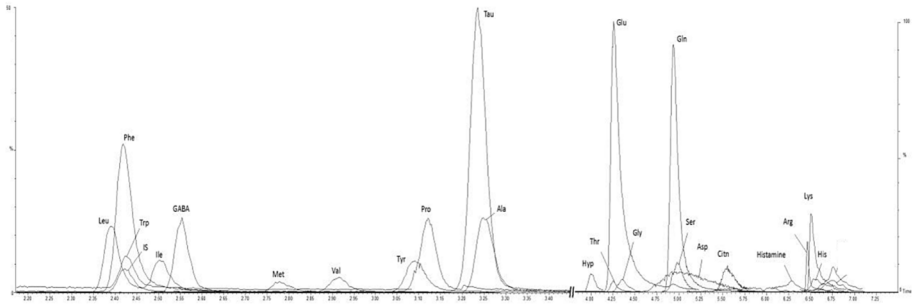

Fig. 2. Typical overlap chromatograms of twenty-three AAs and internal standard.

Table 2
Sensitivity and instrument precisions of twenty-three AAs in ESI^+ mode.

Amino acids	LOD (pg/ml)	LOQ (pg/ml)	Linear range(ng/ml)	r	Precision Intra-day RSD% (n = 6)	Inter-day RSD% (n = 7)
Met	8	80	1.67–107.00	0.999	2.45	2.07
GABA	20	200	17.50–4480.00	0.998	1.44	1.87
Hyp	12	120	0.44–28.25	0.992	1.68	2.85
Gln	5	50	7.38–5670.00	0.994	1.07	2.30
Ala	100	1000	18.28–1170.00	0.998	2.63	2.80
Trp	100	1000	2.41–154.50	0.967	2.37	2.99
Arg	0.006	0.06	2.65–452.00	0.999	0.63	0.87
Phe	0.002	0.06	1.63–156.00	0.998	1.41	2.47
His	350	3500	8.83–565.00	0.999	6.10	2.91
Thr	12	20	9.53–610.00	0.925	0.94	2.72
Asp	1100	5000	55.31–3540.00	0.894	1.77	2.81
Glu	50	25	56.33–11900.00	0.999	5.79	1.93
Pro	0.015	0.015	1.83–117.00	0.999	2.18	1.62
Ile	3.5	35	0.41–78.60	0.998	2.70	1.98
Tau	110	1100	19.22–5535.00	0.999	2.92	2.70
Cit	6	60	0.66–84.00	0.999	1.72	2.04
Val	3.5	35	1.58–101.00	0.999	1.79	2.44
Ser	1.2	12	10.00–960.00	0.999	2.09	2.39
Leu	0.07	0.7	1.80–230.00	0.945	2.18	2.99
Gly	3000	30,000	28.13–1800.00	0.976	2.90	2.45
Lys	2000	0.02	7.56–484.00	0.999	2.89	1.75
Tyr	15	150	1.00–192.00	0.999	2.12	2.09
Histamine	30	300	0.21–13.20	0.999	2.75	1.73

Table 3
Stability, repeatability and recovery of twenty-three AAs in the cortex.

Amino acids	Repeatability RSD%(n = 6)	Accuracy		Stability	
		Average recovery (n = 6)	Recovery RSD%	Freeze-thaw stability RSD% (n = 6)	Short-term stability RSD% (n = 7)
Ala	2.64	91.97	4.76	1.75	4.25
GABA	3.58	94.86	2.82	2.88	4.77
Ser	1.70	105.10	5.37	2.05	3.81
Pro	1.89	90.45	4.67	1.01	2.56
Val	5.18	91.90	5.33	2.19	2.98
Thr	1.73	87.23	3.67	0.79	2.67
Tau	3.25	92.71	4.22	1.59	1.38
Hyp	1.72	91.58	5.04	1.98	4.48
Ile	3.78	92.39	3.96	1.81	3.09
Asp	1.99	99.68	8.47	1.86	1.95
Gln	2.25	96.98	1.72	1.37	3.41
Glu	1.05	84.09	5.03	1.15	2.76
Met	2.64	87.99	5.15	2.25	4.99
His	2.76	88.65	4.12	2.30	3.11
Phe	1.57	90.67	4.11	1.12	2.94
Arg	1.90	91.63	4.32	2.04	4.87
Cit	3.25	94.79	3.38	7.40	4.14
Trp	1.52	97.52	4.38	2.19	4.07
Gly	0.96	94.71	3.84	2.46	1.03
Histamine	4.01	85.90	9.25	4.33	2.90
Leu	1.62	92.09	2.65	1.18	2.50
Lys	2.12	93.85	5.91	3.20	4.54
Tyr	2.28	92.45	2.10	2.38	2.74

corresponding RSD were between 1.72 % and 13.12 %, as shown in Table 3 and 4. The results indicate that the method is accurate and precise enough for the measurement of AAs in the cortex and hippocampus samples.

3.2.3. *Stability and repeatability*

The stabilities of AAs in the cortex and hippocampus samples obtained at the end of the extraction procedure were also assessed. The results of all stability tests are shown in Table 3 and 4. In the short-term stability test of 24 h in 4 °C autosampler after preparation, and the RSD values of all AAs were all within 0.91 % to 11.46 %, suggesting that the sample exhibited high stability in 4 °C autosampler before injection. All the detected AAs in the cortex and hippocampus after three freeze–thaw cycles have the stabilities with RSDs less than 10.94 %. To confirm repeatability, six cortex and hippocampus samples prepared in parallel were analyzed, and the RSD of the twenty-three detected AAs were 0.68–5.18 %. Overall, the results outlined above indicate that this analytical method was accurate as well as stable and reproducible, within acceptable limits and could be used to analyze AAs in the cortex and hippocampus.

3.3. *Dynamic alteration of AAs in the cortex and hippocampus of MCAO rats*

AAs perform critical roles in cell signaling, biosynthesis, transportation, and key metabolic pathways in cerebral ischemia. MCAO typically results in extensive damage to the ischemic cortex and hippocampus. Based on the developed method by LC-QQQ-MS/MS, the contents of twenty-three AAs in the cortex and hippocampus of MCAO rats at 3, 12 and 24 h after occlusion were analyzed. All AAs contents in the different groups are all shown as the mean ± sd in Table S1 (in Supplementary materials).

The cortex is the most sensitive area of cerebral ischemic injury, so we first analyze the dynamic changes of AAs in the cortex(Rho et al., 2018). As shown in Fig. 3A, PCA score plot results showed a marked distinction between the model and sham group at 12 h ($R^2X = 0.63$, $Q^2 = 0.58$) and 24 h ($R^2X = 0.61$, $Q^2 = 0.87$). Compared to 3 h, there is a significant difference in the AAs metabolism profile at 12 and 24 h after ischemia compared to sham group. The neurological function score and TTC staining results in Fig. 1 also indicate more severe brain tissue damage at 12 and 24 h. Based on the above results, we conclude that the brain injury is more severe 12 and 24 h after CI, and the AAs metabolism profile also undergoes significant changes. In order to accurately

Table 4
Stability, repeatability and recovery of twenty-three AAs in the hippocampus.

Amino acids	Repeatability RSD%(n = 6)	Accuracy		Stability	
		Average recovery (n = 6)	Recovery RSD%	Freeze-thaw stability RSD% (n = 6)	Short-term stability RSD% (n = 7)
Ala	2.30	87.23	9.77	2.71	3.45
GABA	0.68	112.25	2.97	0.92	1.07
Ser	0.98	119.77	4.31	2.55	2.92
Pro	0.92	112.78	5.94	4.46	3.64
Val	1.13	92.79	3.48	1.92	3.97
Thr	4.26	109.07	3.01	2.42	0.91
Tau	0.98	87.25	2.18	2.56	1.77
Hyp	3.09	111.76	4.85	6.79	3.80
Ile	1.07	113.33	2.63	1.93	3.74
Asp	3.74	105.89	3.96	2.73	2.13
Gln	1.42	80.00	13.12	2.39	4.81
Glu	0.79	116.69	2.67	2.63	0.93
Met	1.69	91.23	6.54	3.32	2.14
His	0.87	91.40	3.62	5.55	4.87
Phe	1.86	102.18	10.36	1.14	4.65
Arg	3.66	80.47	3.46	5.47	5.36
Cit	4.30	97.96	4.05	10.60	11.46
Trp	1.68	80.46	3.53	2.49	1.32
Gly	3.46	129.08	5.60	2.22	3.64
Histamine	1.57	88.33	2.67	10.94	4.11
Leu	2.55	93.98	3.84	1.74	2.32
Lys	3.05	106.91	3.25	4.35	3.80
Tyr	1.45	80.30	5.34	1.82	1.95

discovery the credible AAs biomarkers related to the development of ischemic injury, the fold-changes (FC) of MCAO group vs. sham group with heatmap analysis was firstly used to filtered the potential biomarkers, those have a continuous and consistent changes at different time points after CI. Then ROC analysis was further conducted to evaluate the diagnostic value of these continuously changing AAs. AUC value of ROC analysis between 0.7 and 0.9 is considered to have a certain discrimination effect.

As shown in Fig. 3B, the heatmap shows the FC of the AAs between MCAO group and sham group at different time points. As shown in the legend, “blue-white-red” represents the dynamic change trend of FC value. Based on the heatmap, a total of thirteen AAs including Ala, Pro, Val, Thr, Hyp, Ile, Gln, His, Arg, Cit, histamine, Leu and Tyr are found to show continuous increases and one AAs of GABA show continuous decreases at different time points after CI. ROC analysis was further conducted to evaluate the diagnostic value of these continuously changing AAs. As shown in Fig. 3C, the AUC of eight AAs including Ala, GABA, Pro, Val, Ile, His, Cit and Leu were all greater than 0.70, which imply these eight AAs would be the AAs biomarkers in cortex, those are closely related to the development of ischemic injury after CI. The detailed information on the contents of these eight AAs in different groups at 3, 12 and 24 h after occlusion is shown in Fig. 3D.

The hippocampus is arguably one of the most plastic regions of the brain(Jurkowski et al., 2020). Hypoxia or ischemia produces elevation in intracellular free calcium concentrations of hippocampal neurons, which leads to neuronal damage and death. Therefore, this study further detected the dynamic changes of AAs in hippocampus. As shown in Fig. 3E, PCA score plot ($R^2X = 0.72$, $Q^2 = 0.98$) showed that AAs is obviously different at 24 h after cerebral ischemia. As shown in Fig. 3F, FC values of three AAs including GABA, Arg and Cit show continuous increases and nine AAs including Ala, Pro, Ile, Asp, Met, His, Phe, Gly and Lys show continuous decreases. Among these changing AAs above, ROC analysis showed that the AUC of three AAs including Asp, Ile, Cit were greater than 0.7 in Fig. 3G, which imply these AAs would be the AAs biomarkers in hippocampus, those are closely related to the development of ischemic injury after CI. The detailed information on the contents of these four AAs at 3, 12 and 24 h after occlusion in different groups is displayed in Fig. 3H.

Taken in concert, the above results show that AAs metabolism is disturbed in the cortex and hippocampus at acute stage of CI. A total of nine AAs biomarkers were finally obtained including eight AAs of Ala, GABA, Pro, Val, Ile, His, Cit and Leu in cortex, and three AAs of Ile, Asp, and Cit in hippocampus. Furthermore, according to the overall changing trends based on PCA scores plot at different time after ischemia, the time of the AAs metabolism showing an obvious disturbance in the cortex (12 and 24 h after ischemia) is earlier than that in the hippocampus (24 h after ischemia). Among the nine AAs metabolic biomarkers discovered in the cortex and hippocampus, Ile and Cit are the common metabolic biomarkers. The levels of Cit increased significantly in both regions of in cortex and hippocampus at 3, 12 and 24 h after ischemia. On the other hand, the level of Ile increased significantly in cortex and decreased significantly in hippocampus at 3, 12 and 24 h after ischemia. The results above fully reflect the spatial–temporal dependence of the AAs in cortex and hippocampus after cerebral ischemia.

To investigate the relationships of the nine AAs biomarkers, we constructed a correlation network diagram based on the KEGG and MetaboAnalyst databases. As shown in Table S3 (in Supplementary materials), under the limiting condition of $P < 0.05$ in the MetaboAnalyst database, there are mainly 4 enriched metabolic pathways in the cortex, including Valine, leucine and isoleucine biosynthesis (BCAAs (branched chain amino acids) biosynthesis); Valine, leucine and isoleucine degradation; Alanine, aspartate and glutamate metabolism and Arginine and proline metabolism. There are 6 main enrichment metabolic pathways in hippocampus, including Arginine biosynthesis; Valine, leucine and isoleucine biosynthesis; Nicotinate and nicotinamide metabolism; Histidine metabolism; Pantothenate and CoA biosynthesis and beta-Alanine metabolism. Among them, four pathways involved in aspartate alone are significantly altered only in the hippocampus. The Valine, leucine and isoleucine metabolism and Arginine metabolism were changed in the cortex and hippocampus.

Recent studies have suggested that BCAAs biosynthesis is associated with a risk of cardiovascular disease and thrombosis(Xu et al., 2020). BCAAs play an important role in the shuttling of nitrogen between organs and tissues, provide nitrogen for neurotransmitter synthesis in the CNS, and are directly associated with endothelial dysfunction through increased reactive oxygen species generation and inflammation(Ma et al., 2022). Furthermore, BCAAs play an important role in the brain, they are integral in the glutamate-glutamine cycle between astrocytes and neurons, which is critical for the efficient uptake of glutamate during excitatory neuronal signaling(Hutson et al., 2001). A study of human participants that compared blood and urine metabolite concentrations in the acute and chronic stages of CI found that serum concentrations of valine, isoleucine, and leucine were significantly elevated in the acute stage(Sidorov et al., 2020). Wang et al(Wang et al., 2013), showed that the level of Ala in cerebrospinal fluid of rats increased significantly 8 h after ischemia, and our results showed that Ala levels increased significantly at 3 h after ischemia and continued to increase until 24 h in the cortex. Previous studies have shown that Ile levels in rat plasma, rat cerebrospinal fluid, and human plasma decreased significantly at 2 h after ischemia(Kimberly et al., 2013), and other studies show that Ile levels in cortex increased significantly at 12 h and 24 h after ischemia(Cui et al., 2018). Our results showed that Ile level was increased in cortex and decreased in hippocampus with the prolongation of ischemic time.

Nitric oxide (NO) produced by Arginine and proline metabolism plays an important role in cardiovascular regulation(Javrushyan et al., 2021). NO regulates blood flow, relaxes blood vessels and inhibits platelet aggregation, and promotes recovery from stroke-related dysfunction(Conti et al., 2013). Arginine metabolism further affects proline metabolism, resulting in a series of downstream effects, such as blocking the cell cycle, autophagy, and apoptosis(Ge et al., 2020; Selen et al., 2015). Cit is a byproduct of the reaction catalyzed by NOS family and produced from Arg. Cit was detected by HMR in the plasma showed

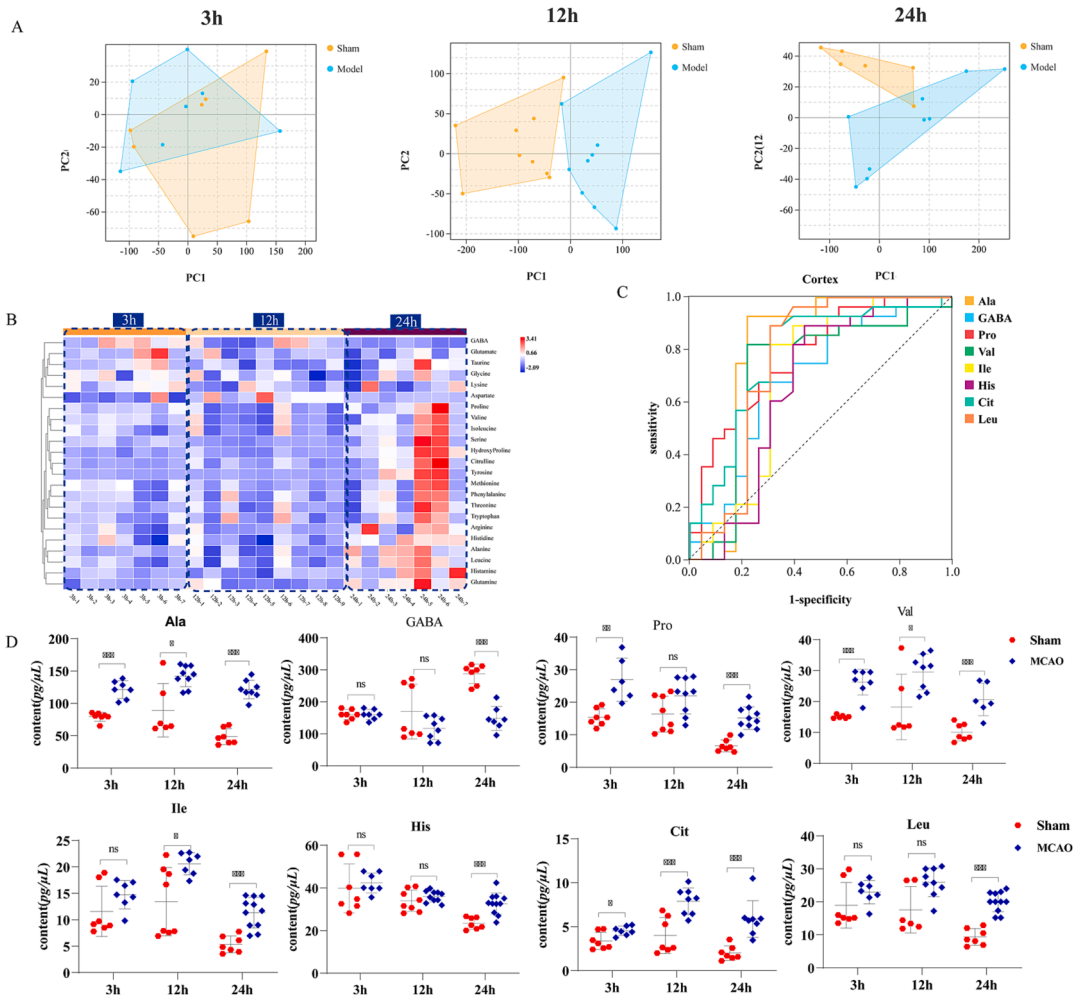

Fig. 3. Dynamic changes in the AAs metabolism profile and screening of time-related AAs of CI. A. The score plot using the first two principal components for the PCA model of sham and MCAO group in the cortex; B. Changes in FC between the model group and sham group at different time points of CI in the cortex; C. ROC curves of candidate markers that could distinguish the model group from the sham group in the cortex; D. Dynamic changes of AAs in cortex closely related to disease evolution; E. The score plot using the first two principal components for the PCA model of sham and MCAO group in the hippocampus; F. Changes in FC between the model group and sham group at different time points of CI in the hippocampus; G. ROC curves of candidate markers that could distinguish the model group from the sham group in the hippocampus; H. Dynamic changes of AAs in hippocampus closely related to disease evolution. $^{*}p < 0.05$, $^{**}p < 0.01$, and $^{***}p < 0.001$.

decreases at 3 h after CI(Baranovicova et al., 2020). In this study showed that Cit increased in the cortex at three time points of 3, 12, 24 h after CI and increased in the hippocampus at 24 h after CI, and may serve as biomarkers for the prediction of CI.

The alanine, aspartate and glutamate metabolism pathways are altered only in cortex. Excessive release of AAs neurotransmitters is regarded as an important pathogenesis mechanism during CI(Oda et al., 2007). This depolarization is mediated by metabolic failure caused by ischemia, and results in the influx of Ca^{2+} via voltage-sensitive Ca^{2+} channels. This causes the excitatory neurotransmitter to become disturbed, inducing a series of events that lead to cell death(Butcher et al., 1990). Ala is a nonessential amino acid that the human body can produce by itself, and it is the main product of pyruvate reduction(Guo et al., 2015). Previous studies have shown that Ala levels in rat cortex increased significantly at 12 h and 24 h after ischemia(Cui et al., 2018), and increased significantly in cerebrospinal fluid at 2 h after ischemia (Wang et al., 2013). Our results showed that Ala levels increased significantly at 3 h after CI and continued to increase until 24 h in the cortex. Asp, is widely distributed in the brain and have been implicated in the pathogenesis of neuronal injury after a variety of central nervous system insults. Many studies have shown that the Asp levels was increased significantly at 12 h and 24 h after CI in whole brain tissue (Yang et al., 2016). However, in this study, Asp shown continuous decreases in the hippocampus at 3, 12, 24 h after CI.

3.4. *NXT achieves neuroprotective effects by regulating AAs metabolism profile in the cortex and hippocampus*

After treatment of NXT, these perturbations of AAs of CI could be partly reversed at different time points after MCAO especially at 24 h after CI. In the cortex area, PCA score plot showed obvious separation between the model and NXT group at 24 h after MCAO ($R^2X = 0.87$, $Q^2 = 0.93$), and an evident district distance was not found at 3 and 12 h in Fig. 4A. In the heatmap of Fig. 4C, the results also show that NXT plays an obvious protective role at 24 h after CI. Among the eight discovered AAs biomarkers in the cortex, four AAs biomarkers of GABA, Pro, His and Leu were significantly changed and close to normal in NXT-treated group compared with model group at 24 h ($P < 0.05$) in Fig. 4E.

Similarly, in the hippocampus, until 24 h after MCAO, an obvious difference can be observed based on PCA score plot of model group and NXT group ($R^2X = 0.50$, $Q^2 = 0.77$) in Fig. 4B. The heatmap results of Fig. 4D show that the perturbations of AAs could be partly reversed at

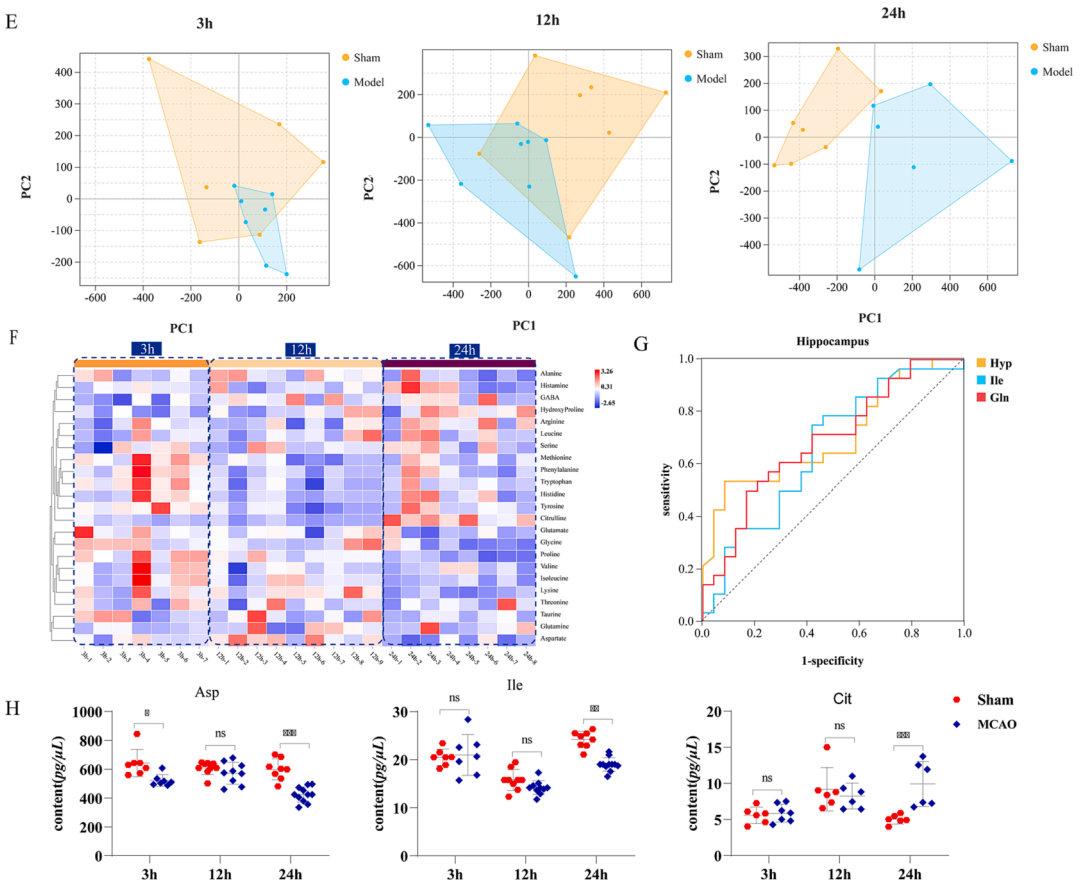

Fig. 3. (*continued*).

24 h after MCAO. Especially, three AAs biomarkers of Asp, Ile and Cit in the hippocampus were found to significantly change in NXT-treated group compared to MCAO group and exhibited an obvious tendency for returning to baseline values after NXT treatment at 24 h after MCAO ($P < 0.05$), shown in Fig. 4F. These findings suggest that the therapeutic effects of NXT on CI were partly due to dynamical interferences with the AAs metabolism in cortex and hippocampus especially at 24 h after CI.

We constructed NXT intervention network diagram based on the KEGG and MetaboAnalyst databases. As shown in Table S4 (in Supplementary materials), under the limiting condition of $P < 0.05$ in the MetaboAnalyst database, there are mainly two enriched metabolic pathways in cortex, including Valine, leucine and isoleucine biosynthesis; Arginine and proline metabolism. There are six enriched metabolic pathways in hippocampus, including Arginine biosynthesis Valine, leucine and isoleucine biosynthesis; Nicotinate and nicotinamide metabolism; Histidine metabolism; Pantothenate and CoA biosynthesis; beta-Alanine metabolism.

4. Conclusion

In this study, a novel analytical method for the detection of twenty-three AAs without derivatization was developed by UPLC-QQQ-MS to analyze the AAs metabolism profiles in cortex and hippocampus and evaluate the therapeutic effects of NXT from the levels of metabolites. The method proved to be rapid, sensitive, accurate, and reproducible within acceptable limits and could be used to analyze AAs in cortex and hippocampus.

Based on a MCAO rat model, the cerebral infarction and the neurological behavior scores are firstly dynamically evaluated at 3, 12, and 24 h after MCAO. The results showed that MCAO rats showed neurological deficits, especially at 24 h. Accordingly, the levels of the twenty-three AAs in cortex and hippocampus at 3, 12, and 24 h after MCAO are dynamically analyzed. An overview based on score plots of PCA showed that with the extension of ischemic time, the distinction observed between MCAO group and sham group became more obvious in the cortex (12 and 24 h after ischemia) and in the hippocampus (24 h after ischemia). The FC values of MCAO group vs. sham group with heatmap analysis was firstly analyzed. The AAs, those have a continuous and consistent changing trends of FC values at different time points after CI are filtered as the potential biomarkers. Then receiver operating curve (ROC) analysis was further conducted to evaluate the diagnostic value of these potential biomarkers and confirm the credible AAs biomarkers related to the development of ischemic injury. As a results, nine AAs biomarkers were finally obtained including eight AAs of Ala, GABA, Pro, Val, Ile, His, Cit and Leu in cortex, and three AAs of Asp, Ile, and Cit in hippocampus. These AAs have obvious continuous and consistent changes at different time points after CI, and it has been reported in the literature that they can affect the occurrence and development of cerebral ischemia through a certain metabolic pathway, and are considered to be important metabolites in the cortex and hippocampus.

After NXT treatment, the efficacy was confirmed by reducing cerebral infarction at 12, 24 h after CI and improving the neurological behavior scores at 3, 12, 24 h after CI. Based on PCA score plots,the obvious distinction observed between MCAO and NXT-treated group in the cortex and hippocampus were both at 24 h after CI. Furthermore, among the nine discovered AAs biomarkers above, GABA, Pro, His, Leu, Asp, Ile and Cit were found to significantly change in NXT-treated group compared to MCAO group and exhibited an obvious tendency for returning to baseline values in the corresponding regions of the cortex or hippocampus at 24 h after CI ($P < 0.05$). In addition, after NXT treatment, there are also some other AAs such as Hyp, Gln, Histamine and so on demonstrating obvious tendency for returning to baseline values at

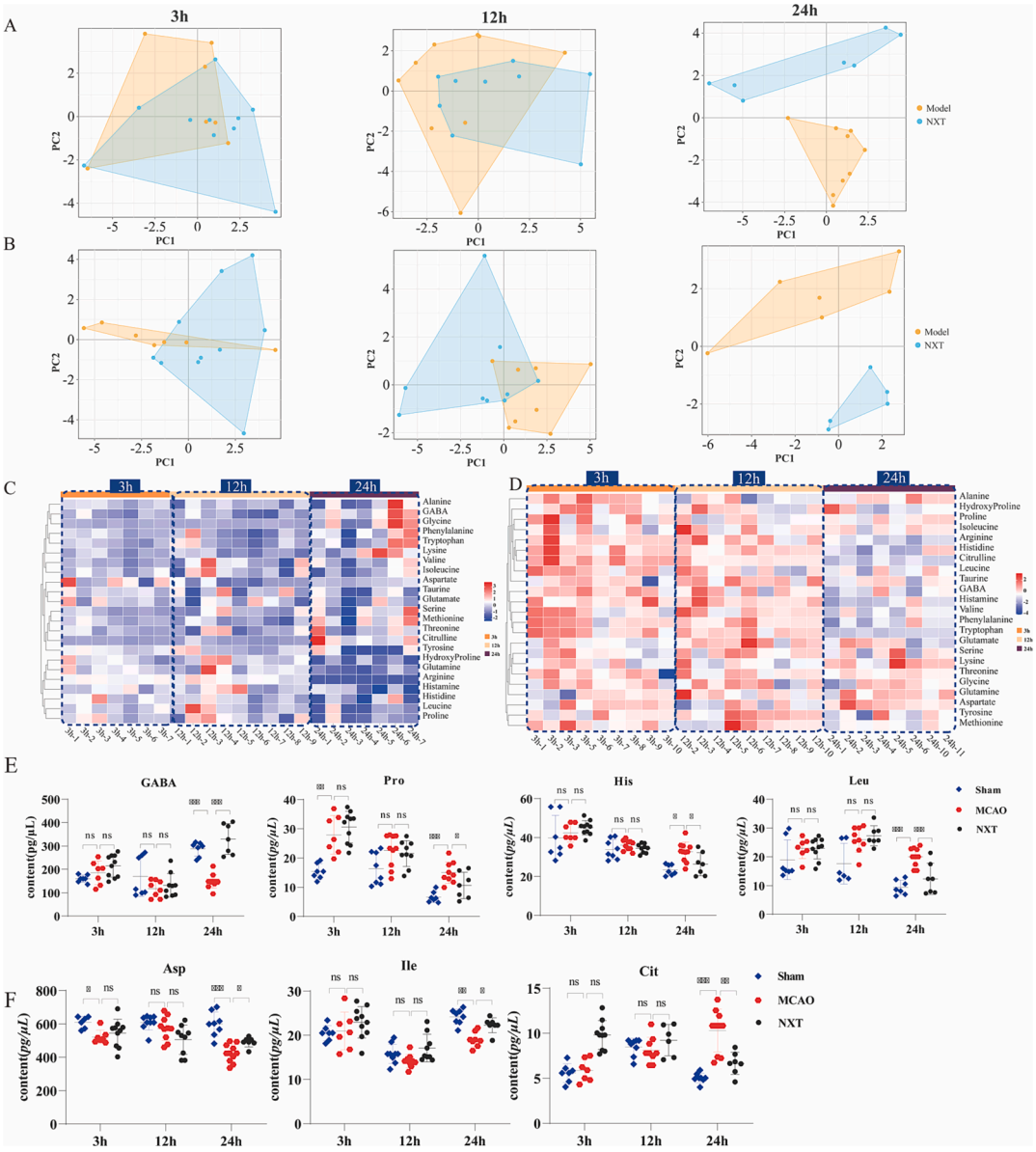

Fig. 4. The therapeutic effect of NXT on CI. A. Score plot using the first two principal components for the PCA model of MCAO and NXT group in the cortex; B. Score plot using the first two principal components for the PCA model of MCAO and NXT group in the hippocampus; C. Changes in AAs FC (NXT treatment vs. Model) in cortex tissues at different time points after NXT treatment; D. Changes in AAs FC (NXT treatment vs. Model) in hippocampal tissues at different time points after NXT treatment; E. Dynamic changes in AAs metabolites that NXT significantly recalled in the cortex; F. Dynamic changes in AAs metabolites that NXT significantly recalled in the hippocampus. $^{*}p < 0.05$, $^{**}p < 0.01$, and $^{***}p < 0.001$.

24 h after CI ($P < 0.05$), which have been detailed in Table S1 (in Supplementary materials). These results suggest that NXT regulates the metabolic profile of AAs in the cortex and hippocampus to achieve neuroprotective effects.

In summary, the developed analytical methods for the detection of AAs provided potential tools for further related disease studies. Moreover, the results obtained throughout this study may help develop novel strategies to explore the dynamic changes of AAs metabolism profiles in cortex and hippocampus after CI and the intervention mechanism of NXT. However, this article only discusses from the perspective of AAs metabolism, and further studies are needed on the upstream enzymes regulating AAs.

Founding.

This study was funded by the Innovative Project in Science and Technology of China Academy of Chinese Medical Sciences (CI2021B017-07, CI2021A05208); National Natural Science Foundation of China (No.81973711); Autonomic Project of China Academy of Chinese Medical Sciences (No. ZXKT22017, ZZ13-019) .

Declaration of competing interest

The authors declare that they have no known competing financial interests or personal relationships that could have appeared to influence the work reported in this paper.

Acknowledgments

We want to thank the participants for taking part in the study.

Appendix A. Supplementary data

Supplementary data to this article can be found online at https://doi.

org/10.1016/j.arabjc.2024.105659.

References

Bame, M., Grier, R.E., Needleman, R., Brusilow, W.S., 2014. Amino acids as biomarkers in the SOD1(G93A) mouse model of ALS. Biochim Biophys Acta 1842, 79–87. https://doi.org/10.1016/j.bbadis.2013.10.004.

Baranovicova, E., Kalenska, D., Tomascova, A., Holubcikova, S., Lehotsky, J., 2020. Time-related metabolomics study in the rat plasma after global cerebral ischemia and reperfusion: effect of ischemic preconditioning. IUBMB Life 72, 2010–2023. https://doi.org/10.1002/iub.2340.

Butcher, S.P., Bullock, R., Graham, D.I., McCulloch, J., 1990. Correlation between amino acid release and neuropathologic outcome in rat brain following middle cerebral artery occlusion. Stroke 21, 1727–1733. https://doi.org/10.1161/01.str.21.12.1727.

Chen, H., Yu, G., Sun, H., Wu, X., Wang, H., 2011. Comparison of adjunctive naoxintong versus clopidogrel in volunteers with the CYP2C19*2 gene mutation accompanied with qi deficiency and blood stasis constitution. Evid Based Complement Alternat Med 2011, 207034. https://doi.org/10.1155/2011/207034.

Chen, H., Zhang, Y., Wu, X., Li, C., Wang, H., 2012. In Vitro assessment of cytochrome P450 2C19 potential of naoxintong. Evid Based Complement Alternat Med 2012, 430262. https://doi.org/10.1155/2012/430262.

Chen, H., Wu, X.Y., Wu, H.X., Wang, H., 2014. A randomized controlled trial of adjunctive bunchang naoxintong Capsule versus maintenance dose clopidogrel in patients with CYP2C19*2 polymorphism. Chin J Integr Med 20, 894–902. https://doi.org/10.1007/s11655-014-2023-z.

Conti, V., Russomanno, G., Corbi, G., Izzo, V., Vecchione, C., Filippelli, A., 2013. Adrenoreceptors and nitric oxide in the cardiovascular system. Front Physiol 4, 321. https://doi.org/10.3389/fphys.2013.00321.

Cui, Y., Wu, H., Liu, M., Yang, H., Qin, H., Liu, X., 2018. Effect of Ginkgo biloba leaf extract on cerebral cortex amino acid levels in cerebral ischemia model rats. Journal of Traditional Chinese Medicine = Chung i Tsa Chih Ying Wen Pan 38, 676–684.

Ge, S., Zhang, Q., Tian, Y., Hao, L., Duan, J., Zhang, B., 2020. Cell metabolic profiling of colorectal cancer via 1H NMR. Clin. Chim. Acta 510, 291–297. https://doi.org/10.1016/j.cca.2020.07.039.

Guan, Q., Liang, S., Wang, Z., Yang, Y., Wang, S., 2014. (1)H NMR-based metabonomic analysis of the effect of optimized rhubarb aglycone on the plasma and urine metabolic fingerprints of focal cerebral ischemia-reperfusion rats. J Ethnopharmacol 154, 65–75. https://doi.org/10.1016/j.jep.2014.03.002.

Guo, Z.L., Zhu, Y., Su, X.T., Liu, J., Yang, Q.X., Nan, J.Y., Zhao, B.C., Zhang, Y.Y., Yu, Y. N., Li, B., Xiao, H.B., Wang, Z., 2015. DanHong injection dose-dependently varies amino acid metabolites and metabolic pathways in the treatment of rats with cerebral ischemia. Acta Pharmacol Sin 36, 748–757. https://doi.org/10.1038/aps.2014.167.

Haiyu, X., Yang, S., Yanqiong, Z., Qiang, J., Defeng, L., Yi, Z., Feng, L., Hongjun, Y., 2016. Identification of key active constituents of Buchang Naoxintong capsules with therapeutic effects against ischemic stroke by using an integrative pharmacology-based approach. Mol Biosyst 12, 233–245. https://doi.org/10.1039/c5mb00460h.

Hutson, S.M., Lieth, E., LaNoue, K.F., 2001. Function of leucine in excitatory neurotransmitter metabolism in the central nervous system. J Nutr 131, 846S–S850. https://doi.org/10.1093/jn/131.3.846S.

Igarashi, H., Suzuki, Y., Huber, V.J., Ida, M., Nakada, T., 2015. N-acetylaspartate decrease in acute stage of ischemic stroke: a perspective from experimental and clinical studies. Magn Reson Med Sci 14, 13–24. https://doi.org/10.2463/mrms.2014-0039.

Jangholi, E., Sharifi, Z.N., Hoseinian, M., Zarrindast, M.R., Rahimi, H.R., Mowla, A., Aryan, H., Javidi, M.A., Parsa, Y., Ghaffarpasand, F., Yadollah-Damavandi, S., Arani, H.Z., Shahi, F., Movassaghi, S., 2020. Verapamil inhibits mitochondria-induced reactive oxygen species and dependent apoptosis pathways in cerebral transient global ischemia/reperfusion. Oxid Med Cell Longev 2020, 5872645. https://doi.org/10.1155/2020/5872645.

Javrushyan, H., Avtandilyan, N., Trchounian, A., 2021. The effects of NO on the urea cycle pathway in short-term intermittent hypobaric hypoxia in rats. Respir Physiol Neurobiol 285, 103598. https://doi.org/10.1016/j.resp.2020.103598.

Jiang, J., Yu, Y., 2021. Small molecules targeting cyclooxygenase/prostanoid cascade in experimental brain ischemia: do they translate? Med Res Rev 41, 828–857. https://doi.org/10.1002/med.21744.

Jurkowski, M.P., Bettio, L.K., Woo, E., Patten, A., Yau, S.Y., Gil-Mohapel, J., 2020. Beyond the hippocampus and the SVZ: adult neurogenesis throughout the brain. Front Cell Neurosci 14, 576444. https://doi.org/10.3389/fncel.2020.576444.

Kimberly, W.T., Wang, Y., Pham, L., Furie, K.L., Gerszten, R.E., 2013. Metabolite profiling identifies a branched chain amino acid signature in acute cardioembolic stroke. Stroke 44, 1389–1395. https://doi.org/10.1161/STROKEAHA.111.000397.

Klacanova, K., Kovalska, M., Chomova, M., Pilchova, I., Tatarkova, Z., Kaplan, P., Racay, P., 2019. Global brain ischemia in rats is associated with mitochondrial release and downregulation of Mfn2 in the cerebral cortex, but not the hippocampus. Int. J. Mol. Med. 43, 2420–2428. https://doi.org/10.3892/ijmm.2019.4168.

Liang, Q., Cai, Y., Chen, R., Chen, W., Chen, L., Xiao, Y., 2018. The effect of naoxintong capsule in the treatment of patients with cerebral infarction and carotid atherosclerosis: a systematic review and meta-analysis of randomized trials. Evid Based Complement Alternat Med 2018, 5892306. https://doi.org/10.1155/2018/5892306.

Liu, M., Liu, X., Wang, H., Xiao, H., Jing, F., Tang, L., Li, D., Zhang, Y., Wu, H., Yang, H., 2016a. Metabolomics study on the effects of Buchang Naoxintong capsules for treating cerebral ischemia in rats using UPLC-Q/TOF-MS. J Ethnopharmacol 180, 1–11. https://doi.org/10.1016/j.jep.2016.01.016.

Liu, M., Tang, L., Liu, X., Fang, J., Zhan, H., Wu, H., Yang, H., 2016b. An evidence-based review of related metabolites and metabolic network research on cerebral ischemia. Oxid Med Cell Longev 2016, 9162074. https://doi.org/10.1155/2016/9162074.

Longa, E.Z., Weinstein, P.R., Carlson, S., Cummins, R., 1989. Reversible middle cerebral artery occlusion without craniectomy in rats. Stroke 20, 84–91. https://doi.org/10.1161/01.str.20.1.84.

Ma, H.-F., Zheng, F., Su, L.-J., Zhang, D.-W., Liu, Y.-N., Li, F., Zhang, Y.-Y., Gong, S.-S., Kou, J.-P., 2022. Metabolomic profiling of brain protective effect of edaravone on cerebral ischemia-reperfusion injury in mice. Front Pharmacol 13, 814942. https://doi.org/10.3389/fphar.2022.814942.

Mitani, A., Yanase, H., Sakai, K., Wake, Y., Kataoka, K., 1993. Origin of intracellular Ca2 + elevation induced by in vitro ischemia-like condition in hippocampal slices. Brain Res. 601, 103–110. https://doi.org/10.1016/0006-8993(93)91700-3.

Muir, K.W., Lees, K.R., 2003. Excitatory amino acid antagonists for acute stroke. Cochrane Database Syst Rev CD001244. https://doi.org/10.1002/14651858.CD001244.

Oda, M., Kure, S., Sugawara, T., Yamaguchi, S., Kojima, K., Shinka, T., Sato, K., Narisawa, A., Aoki, Y., Matsubara, Y., Omae, T., Mizoi, K., Kinouchi, H., 2007. Direct correlation between ischemic injury and extracellular glycine concentration in mice with genetically altered activities of the glycine cleavage multienzyme system. Stroke 38, 2157–2164. https://doi.org/10.1161/STROKEAHA.106.477026.

Rho, H.J., Kim, J.H., Lee, S.H., 2018. Function of selective neuromodulatory projections in the mammalian cerebral cortex: comparison between cholinergic and noradrenergic systems. Front Neural Circuits 12, 47. https://doi.org/10.3389/fncir.2018.00047.

Selen, E.S., Bolandnazar, Z., Tonelli, M., Bütz, D.E., Haviland, J.A., Porter, W.P., Assadi-Porter, F.M., 2015. NMR metabolomics show evidence for mitochondrial oxidative stress in a mouse model of polycystic ovary syndrome. J Proteome Res 14, 3284–3291. https://doi.org/10.1021/acs.jproteome.5b00307.

Sidorov, E., Bejar, C., Xu, C., Ray, B., Reddivari, L., Chainakul, J., Vanamala, J.K.P., Sanghera, D.K., 2020. Potential metabolite biomarkers for acute versus chronic stage of ischemic stroke: a pilot study. J Stroke Cerebrovasc Dis 29, 104618. https://doi.org/10.1016/j.jstrokecerebrovasdis.2019.104618.

Song, Y., Xu, C., Kuroki, H., Liao, Y., Tsunoda, M., 2018. Recent trends in analytical methods for the determination of amino acids in biological samples. J Pharm Biomed Anal 147, 35–49. https://doi.org/10.1016/j.jpba.2017.08.050.

Wahul, A.B., Joshi, P.C., Kumar, A., Chakravarty, S., 2018. Transient global cerebral ischemia differentially affects cortex, striatum and hippocampus in Bilateral Common Carotid Arterial occlusion (BCCAo) mouse model. J Chem Neuroanat 92, 1–15. https://doi.org/10.1016/j.jchemneu.2018.04.006.

Wang, X., Lin, F., Gao, Y., Lei, H., 2015. Bilateral common carotid artery occlusion induced brain lesions in rats: a longitudinal diffusion tensor imaging study. Magn Reson Imaging 33, 551–558. https://doi.org/10.1016/j.mri.2015.02.010.

Wang, Y., Wang, Y., Li, M., Xu, P., Gu, T., Ma, T., Gu, S., 2013. (1)H NMR-based metabolomics exploring biomarkers in rat cerebrospinal fluid after cerebral ischemia/reperfusion. Mol Biosyst 9, 431–439. https://doi.org/10.1039/c2mb25224d.

Wang, P.R., Wang, J.S., Yang, M.H., Kong, L.Y., 2014. Neuroprotective effects of Huang-Lian-Jie-Du-Decoction on ischemic stroke rats revealed by (1)H NMR metabolomics approach. J Pharm Biomed Anal 88, 106–116. https://doi.org/10.1016/j.jpba.2013.08.025.

Woitzik, J., Schneider, U.C., Thome, C., Schroeck, H., Schilling, L., 2006. Comparison of different intravascular thread occlusion models for experimental stroke in rats. J Neurosci Methods 151, 224–231. https://doi.org/10.1016/j.jneumeth.2005.07.007.

Xing, C., Arai, K., Lo, E.H., Hommel, M., 2012. Pathophysiologic cascades in ischemic stroke. Int J Stroke 7, 378–385. https://doi.org/10.1111/j.1747-4949.2012.00839.x.

Xu, Y., Jiang, H., Li, L., Chen, F., Liu, Y., Zhou, M., Wang, J., Jiang, J., Li, X., Fan, X., Zhang, L., Zhang, J., Qiu, J., Wu, Y., Fang, C., Sun, H., Liu, J., 2020. Branched-chain amino acid catabolism promotes thrombosis risk by enhancing tropomodulin-3 propionylation in platelets. Circulation 142, 49–64. https://doi.org/10.1161/CIRCULATIONAHA.119.043581.

Yamori, Y., Horie, R., Handa, H., Sato, M., Fukase, M., 1976. Pathogenetic similarity of strokes in stroke-prone spontaneously hypertensive rats and humans. Stroke 7, 46–53. https://doi.org/10.1161/01.str.7.1.46.

Yang, R., Chen, K., Zhao, Y., Tian, P., Duan, F., Sun, W., Liu, Y., Yan, Z., Li, S., 2016. Analysis of potential amino acid biomarkers in brain tissue and the effect of galangin on cerebral ischemia. Molecules 21. https://doi.org/10.3390/molecules21040438.

Zhang, F., Huang, B., Zhao, Y., Tang, S., Xu, H., Wang, L., Liang, R., Yang, H., 2013. BNC protects H9c2 cardiomyoblasts from H 2 O 2 -induced oxidative injury through ERK1/2 signaling pathway. Evid Based Complement Alternat Med 2013, 802784. https://doi.org/10.1155/2013/802784.

Zhao, S., Tang, Y., Cai, H., Liu, W., Zhang, L., Chen, D., Chen, B., 2018. Treatment of danhong injection combined with naoxintong capsule in acute coronary syndrome patients undergoing PCI operation: study for a randomized controlled and double-blind trial. Evid Based Complement Alternat Med 2018, 8485472. https://doi.org/10.1155/2018/8485472.

Zhong, X.N., Wang, H.H., Lu, Z.Q., Dai, Y.Q., Huang, J.H., Qiu, W., Shu, Y.Q., Xu, W., Cheng, C., Hu, X.Q., 2013. Effects of Naoxintong on atherosclerosis and inducible

nitric oxide synthase expression in atherosclerotic rabbit. Chin Med J (Engl) 126, 1166–1170.

Zhou, Z., Lu, J., Liu, W.W., Manaenko, A., Hou, X., Mei, Q., Huang, J.L., Tang, J., Zhang, J.H., Yao, H., Hu, Q., 2018. Advances in stroke pharmacology. Pharmacol Ther 191, 23–42. https://doi.org/10.1016/j.pharmthera.2018.05.012.

Zhu, Y., Guo, Z., Zhang, L., Zhang, Y., Chen, Y., Nan, J., Zhao, B., Xiao, H., Wang, Z., Wang, Y., 2015. System-wide assembly of pathways and modules hierarchically reveal metabolic mechanism of cerebral ischemia. Sci Rep 5, 17068. https://doi.org/10.1038/srep17068.